

MODELLING THE INTERACTIONS OF SICKLE CELL GENE ON MALARIA TRANSMISSION DYNAMICS

R. I. GWERYINA, O. ABAH AND F. S. KADUNA

ABSTRACT. This article proposes a deterministic three-dimensional system for the transmission dynamics of malaria in a mosquito and genetically stratified human populations. To assess the impact of intervention measures, we derive a formula for the basic reproduction number, R_i of infection and examine the existence of infection endemic equilibria. The model is found to exhibit backward bifurcation (where the infection-free and infection endemic equilibria co-exist), with this situation, the usual epidemiological condition of malaria elimination among each genotype population, $R_i < 1$, is no longer sufficient, even though necessary. The model is also shown to undergo a Hopf bifurcation under certain conditions. Further, the infection-free equilibrium is shown to be stable globally in the instance $R_i < 1$ and on the condition that there are no persisting mosquito bites in the population. The global stability of infection endemic equilibrium is also studied when the basic reproduction number is greater than unity. Finally, we provide numerical simulations to illustrate our analytical findings with brief discussion.

1. INTRODUCTION

Malaria, an evolutionary driving force behind sickle cell anaemia, is a mosquito-borne disease caused by a parasite of the genus *Plasmodium* from the protozoa group. Its transmission to humans is initiated through bites from infected female *Anopheles* mosquitoes. *Plasmodium falciparum* as a leading cause of malaria is estimated to account for half a billion episodes of the disease each year [2]. More than 7 million infants are the sufferers of sickle cell disease each year globally [20] with 200,000 and above cases in Africa. Nigeria alone has about 150,000 children born annually with sickle cell anaemia [26].

Apart from children under the age of 5 years and the pregnant women with the normal haemoglobin, the sickle cell carriers are the next most vulnerable candidates to malaria related deaths. Even though, many sufferers of sickle cell disease die before the age of 20, modern treatment regimens can now prolong their life cycle up to 40 or more years [8, 21, 23]. Treatment of sickle cell anaemia is usually

2010 *Mathematics Subject Classification.* 92B05, 34D23, 34C25.

Key words and phrases. Sickle cell gene, Malaria, Basic reproduction number, Backward bifurcation, Hopf bifurcation, Global stability.

Submitted Sep. 3, 2020. Revised Jan. 8, 2021.

aimed at avoiding crisis, relieving symptoms and preventing further complications [26]. With the outbreak of Corona virus disease 2019, screening and treatment of malaria in sickle cell carriers has become a matter of complexity since both diseases shared similar symptoms [3, 16].

The genetic content of every child has two copies of haemoglobin one from the mother and the other from the father. When both copies are normal, and mutated genes, then the child is homozygous for HbAA (AA genotype) and HbSS (S-allele) respectively. The latter usually suffers for Sickle cell anemia and unfortunately dies before reaching the adulthood. However, when an inherited gene is mutated and singleton, such person is heterozygous for HbAS (AS genotype), which is formally regarded as the sickle cell carriers. Based on biological analysis, carriers parents has 50% chance to produce a generation with the same trait (AS), a 25% chance of reproducing a generation with both normal haemoglobin (AA) and of course 25% probability of giving out a generation with both S-alleles (SS genotype)[22]. The comparative advantage of S allele individuals is that they acquired more immunity against plasm-odium malaria and plasm-odium faelciparum. As a result, malarial induced death is less in them than those with AS genotype [26]. An elaborate review on these two infections can be traced in [13].

Modelling malaria now is not a novelty in the epidemiological world as this has being done in the early 1911 by Ross Donald. All recent mathematical models on malaria transmission are built on the Ross's foundation, notably[4, 9, 24, 27]. However, examining the malaria and sickle cell gene interactions mathematically is not popularized. Few works actually consider this situation as in [5]-[7] and[12, 18]. [18] modelled the dynamical behaviour of sickle cell anaemia and malaria, but neglected the SS genotype individuals in the formulation on the assumption that the calibre of individuals do not grow up to the reproductive age due to malaria related deaths.

The author recommends the inclusion of such individuals in complex models; and that recommendation gave rise to the present study. We disclaim the earlier assumption and extend the model by incorporating individuals of S-allele since they can survive up to the reproductive stage, and this is the main factor excluded in the past works.

The paper is organized as follows: In the next section, we introduce the model construction and equations in section 2. Stability analysis of the proposed model is done in section 3 while section 4 presented numerical results and discussion. Finally, we conclude the paper in section 5.

2. MODEL DERIVATION

2.1. Model description. The extended model is rooted wholly on the Nakakawa model [18] assumptions except that the present study introduces the population of sickle cell carriers; who in contemporary society can survive up to the reproductive age. The total human population at time t , denoted by $N_h(t)$, is stratified into three classes (based on AA (i=1), AS (i=2) and SS (i=3) genotypes), namely: Susceptible humans (S_i), Infected humans (I_i) and Recovered humans (R_i). Similarly, the total mosquito population at time t , denoted by ($N_m(t)$), is also divided into two

compartments: Susceptible mosquitoes (S_m) and Infected mosquitoes (I_m). Thus,

$$N_h = \sum_{i=1}^3 (S_i + I_i + R_i),$$

$$N_m = S_m + I_m.$$

The susceptible population (for both humans and mosquitoes) are recruited into the population at a rate Δ_i and Δ_m for the human and mosquito population, respectively. Susceptible humans acquire malaria infection and become infected, following effective contact with infected mosquitoes, at a rate λ_h , given by

$$\lambda_h = (1 - p) \frac{\theta_i a(I_m)}{N_h}. \tag{1}$$

Similarly, susceptible mosquitoes acquire malaria following effective bite with infected humans at a rate λ_m , given by

$$\lambda_m = a\phi_i \frac{\sum_{i=1}^3 (I_i + \epsilon R_i)}{N_h}. \tag{2}$$

From (1) and (2), a refers to the biting rate per human per mosquito, p , $0 \leq p \leq 1$ is the human modification parameter that accounts for the protection offered against mosquito bite, θ_i and ϕ_i are the probabilities of transmitting malaria from mosquito-to-human and human-to-mosquito, respectively. ϵ on the other hand is the transmitting rate of malaria to mosquitoes (at reduced factor) by recovered humans. We assume that malaria infected humans gain partial immunity against the disease at a rate γ_i for each i genotype (such that $\gamma_1 < \gamma_2 < \gamma_3$); and recovers at a rate η_i as a result of treatment. Meanwhile, the recovered humans loss immunity at κ_i rate for i genotype. In addition, μ_1 and μ_2 are the natural mortality rates for the human and mosquito population, respectively. Malaria induced death occurs in humans at a rate δ_1 while mosquito mortality rate δ_2 is as a result of human intervention.

To this effect, we also make use of the flow diagram in Figure 1 to derive the couple-system of differential equations

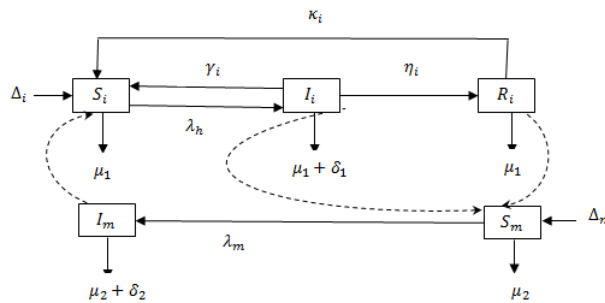


FIGURE 1. Flow diagram for transmission dynamics of malaria

2.2. **The Model.** Putting the above formulation and assumptions together gives the following autonomous system of differential equations

$$\left. \begin{aligned} \frac{dS_i}{dt} &= \Delta_i - (\mu_1 + \lambda_h)S_i + \gamma_i I_i + \kappa_i R_i \\ \frac{dI_i}{dt} &= \lambda_h S_i - (\mu_1 + \delta_1 + \gamma_i + \eta_i)I_i \\ \frac{dR_i}{dt} &= \eta_i I_i - (\mu_1 + \kappa_i)R_i \end{aligned} \right\} \quad (3)$$

for $i = 1, 2, 3$ represents the equations for AA, AS and SS genotype classes respectively. Note that the basic model [18] is obtained at $i = 1, 2$ only

In terms of the mosquito population, we get

$$\left. \begin{aligned} \frac{dS_m}{dt} &= \Delta_m - (\mu_2 + \lambda_m)S_m \\ \frac{dI_m}{dt} &= \lambda_m S_m - (\mu_2 + \delta_2)I_m \end{aligned} \right\} \quad (4)$$

From the systems (3) and (4), we have

$$\left. \begin{aligned} \frac{dN_h}{dt} &= \Delta_i - \mu_i N_h - \delta_1 I_i \\ \frac{dN_m}{dt} &= \Delta_m - \mu_2 N_m - \delta_2 I_m \end{aligned} \right\} \quad (5)$$

where the meaning of the parameters is summarized in the Table 1.

The mathematical well-posedness of the three-dimensional system (3) and (4) can be proved within the domain

$$\Omega = \Omega_h \times \Omega_m, \quad (6)$$

where

$$\Omega_h = \{(S_i, I_i, R_i) \in R_+^3 : N_h \leq \frac{\Delta_i}{\mu_1}\} \text{ for each } i.$$

$$\Omega_m = \{(S_m, I_m) \in R_+^2 : N_m \leq \frac{\Delta_m}{\mu_2}\}$$

TABLE 1. Variables and parameters of the extended model

Variables	Definition
$i = 1$	Individuals of AA genotype
$i = 2$	Individuals of AS genotype
$i = 3$	Individuals of SS genotype
$S_i(t)$	Number of individuals of i genotype susceptible to malaria at time t
$I_i(t)$	Number of individuals of i genotype infected by malaria at time t
$R_i(t)$	Number of individuals of i genotype recovered from malaria at time t
$S_m(t)$	Number of mosquitoes susceptible to the infectious plasmodium parasite at time t
$I_m(t)$	Number of mosquitoes infected by plasmodium parasite at time t
Parameters	Definition
Δ_i	Recruitment rate of susceptible humans of i genotype
Δ_m	Recruitment rate of susceptible mosquitoes
γ_i	Partial immunity of individuals of i genotype against malaria ($\gamma_1 < \gamma_2 < \gamma_3$)
η_i	Recovery rate of individuals of i genotype from malaria due to treatment
κ_i	Rate of immunity loss in individuals of i genotype
μ_1	Human natural mortality rate
μ_2	Mosquito natural mortality rate
δ_1	Human mortality rate due to malaria
δ_2	Mosquito mortality rate due to human intervention
λ_h	Force of infection in human population
λ_m	Force of infection in mosquito population
a	Biting rate per human per mosquito
θ_i	Probability that an individual of type i ($\theta_1 > \theta_2 > \theta_3$) acquires plasmodium per bite
ϕ_i	Probability that a mosquito acquires plasmodium from biting an infected individual of genotype i ($\phi_1 > \phi_2 > \phi_3$)
ϵ	Reduced transmission factor of recovered individuals ($0 < \epsilon < 1$)
p	Human protection parameter against mosquito bite

3. ANALYSIS OF THE EXTENDED MODEL

3.1. **Existence of the equilibria.** Let $E_i^* = (S_i^*, I_i^*, R_i^*)$ be the infection endemic equilibria for the i genotype population of the three-dimensional system (3). Then solving the system at the steady state yields

$$\left. \begin{aligned} S_i^* &= \frac{q_i \Delta_i \hat{\psi}_i}{\mu_1 q_i \hat{\psi}_i + Q_i \lambda_h^*} \\ I_i^* &= \frac{q_i \Delta_i \lambda_h^*}{\mu_1 q_i \hat{\psi}_i + Q_i \lambda_h^*} \\ R_i^* &= \frac{\eta_i \Delta_i \lambda_h^*}{\mu_1 q_i \hat{\psi}_i + Q_i \lambda_h^*} \end{aligned} \right\} \tag{7}$$

such that

$$N_h^* = \frac{q_i \Delta_i \hat{\psi}_i + \lambda_h^* \Delta_i (q_i + \eta_i)}{\mu_1 q_i \hat{\psi}_i + Q_i \lambda_h^*} \tag{8}$$

where $\hat{\psi}_i = \gamma_i + \eta_i + \mu_1 + \delta_1$, $q_i = \mu_1 + \kappa_i$, $Q_i = \mu_1(\mu_1 + \delta_1 + \eta_i) + \kappa_i(\mu_1 + \delta_1)$.

The same procedure yielded $E_m^* = (S_m^*, I_m^*)$ for the mosquito population as given

$$\left. \begin{aligned} S_m^* &= \frac{\Delta_m}{\mu_2 + \lambda_m^*} \\ I_m^* &= \phi_m \frac{\lambda_m^*}{\mu_2 + \lambda_m^*}, \phi_m = \frac{\Delta_m}{\mu_2 + \delta_2} \end{aligned} \right\} \tag{9}$$

But, the forces of infection at this point defines

$$\lambda_m^* = a \phi_i \Delta_i \frac{(q_i + \epsilon \eta_i) \lambda_h^*}{N_h^* (\mu_1 q_i \hat{\psi}_i + Q_i \lambda_h^*)} \tag{10}$$

and

$$\lambda_h^* = (1 - p) \frac{a \theta_i \phi_m}{N_h^*} \left(\frac{\lambda_m^*}{\mu_2 + \lambda_m^*} \right) \tag{11}$$

Thus, using equations (10) and (11), we have

$$\lambda_h^* (a_2 (\lambda_h^*)^2 + a_1 \lambda_h^* + a_0) = 0 \tag{12}$$

Clearly, $\lambda_h^* = 0$ and the infection-free equilibrium (IFE) is

$$\left. \begin{aligned} E_i^0 &= (S_i^0, I_i^0, R_i^0) \\ E_m^0 &= (S_m^0, I_m^0) \end{aligned} \right\} \tag{13}$$

where

$$S_i^0 = \frac{\Delta_i}{\mu_1}, I_i^0 = R_i^0 = 0 \text{ for each } i$$

and

$$S_m^0 = \frac{\Delta_m}{\mu_2} \text{ with } I_m^0 = 0.$$

However, the disease persists when $\lambda_h^* \neq 0$ in (12) to derive the infection endemic equilibrium (IEE) which means that

$$a_2 (\lambda_h^*)^2 + a_1 \lambda_h^* + a_0 = 0, \tag{14}$$

where

$$a_2 = \mu_2 \Delta_i (q_i + \eta_i)^2 + a \phi_i \Delta_i (q_i + \eta_i) (q_i + \epsilon \eta_i)$$

$$a_1 = \mu_2 q_i \hat{\psi}_i \Delta_i (q_i + \eta_i) \left(2 - R_i^2 \frac{Q_i}{\mu_1 (q_i + \eta_i)} \right) + a q_i \phi_i \hat{\psi}_i \Delta_i (q_i + \epsilon \eta_i)$$

and

$$a_0 = \mu_2 \Delta_i q_i^2 \hat{\psi}_i^2 (1 - R_i^2), \tag{15}$$

where

$$R_i = \rho(FV^{-1}) = \sqrt{\frac{(1-p)a^2 \theta_i \phi_i \phi_m \mu_1}{\Delta_i \mu_2 \hat{\psi}_i} (1 + \epsilon \left(\frac{\eta_i}{q_i}\right))} \tag{16}$$

is being derived from the famous next generation operator as explored in [25]. In equation (16) $i = 1, 2, 3$ refers to the basic reproduction ratios in a population of only AA, AS and SS individuals respectively. Note that F and V are

$$F = \begin{pmatrix} 0 & 0 & (1-p)a\theta_i \left(\frac{S_i^0}{N_h^0}\right) \\ 0 & 0 & 0 \\ a\phi_i \left(\frac{S_m^0}{N_h^0}\right) & a\epsilon \left(\frac{S_m^0}{N_h^0}\right) & 0 \end{pmatrix} \quad \text{and} \quad V = \begin{pmatrix} \hat{\psi}_i & 0 & 0 \\ -\eta_i & q_i & 0 \\ 0 & 0 & \mu_2 + \delta_2 \end{pmatrix}$$

with $\frac{S_m^0}{N_h^0} = \frac{S_m^0}{S_i^0} = \frac{\mu_1}{\mu_2} \left(\frac{\Delta_m}{\Delta_i}\right)$.

From equation (14) we can observed that the model has:

- (a) a unique disease equilibrium if $a_0 < 0 \iff R_i > 1$
- (b) a unique disease equilibrium if $a_1 < 0$ and $a_0 < 0$ or $a_1^2 - 4a_2a_0 = 0$
- (c) a dual disease equilibria if $a_1 < 0$, $a_0 > 0$ and $a_1^2 - 4a_2a_0 = 0$
- (d) no disease equilibrium in case the above conditions fail.

The situation in (c) shows the indices of backward bifurcation by quadratic equation method [14] for the system (3) when $R_i < 1$. The phenomenon is demonstrated using the parameter set of values in Table 2, with the result given in Figure 2.

3.2. Local dynamics of the three-dimensional system 3 at the unique infection endemic equilibrium.

Prop. 1 The unique endemic equilibrium E_i^* for the three-dimensional system 3 is locally stable if $R_i > 1$ for each i .

Proof. The Jacobian matrix of the three-dimensional system 3 at the infection endemic equilibrium is

$$Df^i = \begin{pmatrix} -(\mu + \frac{(1-p)a\theta_i I_m}{N_h}) & \gamma_i + S_i \left(\frac{(1-p)a\theta_i I_m}{N_h^2}\right) & \kappa_i + S_i \left(\frac{(1-p)a\theta_i I_m}{N_h^2}\right) \\ \frac{(1-p)a\theta_i I_m}{N_h} & -(\mu_1 + \delta_1 + \gamma_i + \eta_i + S_i \left(\frac{(1-p)a\theta_i I_m}{N_h^2}\right)) & -\left(\frac{(1-p)a\theta_i I_m}{N_h^2}\right) S_i \\ 0 & \eta_i & -(\mu_1 + \kappa_i) \end{pmatrix} \tag{17}$$

with the associated second additive compound matrix denoted by $Df_{[2]}^i$ as given

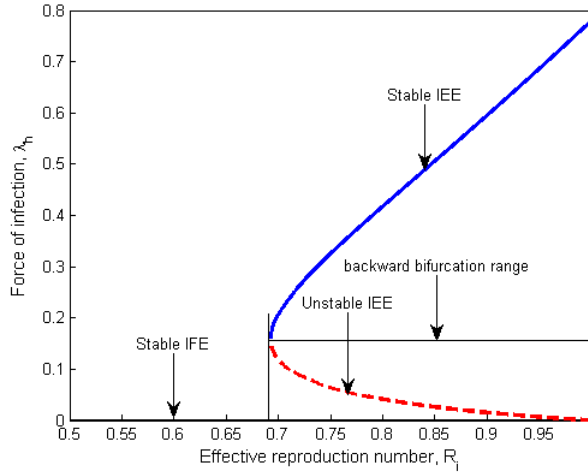


FIGURE 2. backward bifurcation diagram of the three-dimensional system 3. Parameter values used are: $\eta_i = 0.022, \gamma_i = 0.0005, \kappa_i = 0.7, \epsilon = 0.000005; \mu_2 = 0.04; \delta_1 = 0.02, \Delta_i = 7; \Delta_m = 269, p = 0.0$ such that $R_i = 0.8712536993$. All other parameters as in Table 2

$$Df_{[2]}^i = \begin{pmatrix} -(\xi_i + \frac{(1-p)a\theta_i I_m}{N_h}(1 + \frac{S_i}{N_h})) & -S_i(\frac{(1-p)a\theta_i I_m}{N_h^2}) & -(\kappa_i + S_i(\frac{(1-p)a\theta_i I_m}{N_h^2})) \\ \eta_i & -(2\mu_1 + \kappa_i) & \gamma_i + S_i(\frac{(1-p)a\theta_i I_m}{N_h^2}) \\ 0 & \frac{(1-p)a\theta_i I_m}{N_h} & -(\xi_i + S_i(\frac{(1-p)a\theta_i I_m}{N_h^2})) \end{pmatrix} \tag{18}$$

with $\xi_i = 2\mu_1 + \delta_1 + \gamma_i + \eta_i$.

Therefore, it is clear that the trace and determinant of (17) are respectively define as

$$tra(Df^i(E_i^*)) = -(3\mu_1 + \delta_1 + \gamma_i + \eta_i + \kappa_i + \frac{(1-p)a\theta_i I_m}{N_h}(1 + \frac{S_i}{N_h})) < 0$$

and

$$\begin{aligned} det(Df^i(E_i^*)) &= -\frac{(1-p)a\theta_i I_m}{N_h}(\mu + \kappa_i)[\eta_i\mu_1(1 + \frac{S_i}{N_h}) + \mu_1 + \delta_1 + \gamma_i + \eta_i] \\ &= \mu_1[\eta_i\mu_1 + (\mu_1 + \delta_1)(\mu + \kappa_i)] - (1 - \mu_1)[\eta_i\kappa_i + \gamma_i(\mu + \kappa_i)] < 0 \end{aligned}$$

since $\mu_1 < 1$

Similarly

$$\begin{aligned} det(Df_{[2]}^i(E_i^*)) &= -(\xi_i + \frac{(1-p)a\theta_i I_m}{N_h}(1 + \frac{S_i}{N_h}))[(2\mu_1 + \kappa_i)(\xi_i + \frac{(1-p)a\theta_i I_m}{N_h}S_i) \\ &+ \frac{(1-p)a\theta_i I_m}{N_h}(\mu_1 + \delta_1 + \gamma_i + \eta_i)] - \eta_i[\xi_i S_i(\frac{(1-p)a\theta_i I_m}{N_h^2}) + [S_i(\frac{(1-p)a\theta_i I_m}{N_h^2})]^2] \\ &+ \frac{(1-p)a\theta_i I_m}{N_h}(\kappa_i + S_i(\frac{(1-p)a\theta_i I_m}{N_h^2})) < 0 \end{aligned}$$

It is evident from lemma 3 of [17] that the result in prop.1 holds

3.3. Existence of Hopf bifurcation for the three-dimensional system 3 at the infection endemic equilibrium. Hopf bifurcation occurs generally, when the Jacobian of the system evaluated at IEE has a pair of pure imaginary eigenvalues. This is investigated in the following theorem.

Theorem 1: Let $R_i > 1$. Then the infection endemic equilibrium can become unstable through a Hopf bifurcation resulting to an oscillatory solution of the system(3) if

$$p = p^* = 1 - \left(\frac{-\beta \pm \sqrt{\beta^2 - 4\tau\alpha}}{2\tau} \right), \quad (19)$$

where

$$\begin{aligned} \alpha &= (2\mu_1 + \delta_1 + \gamma_i + \eta_i + \kappa_i)[\mu_1(3\mu_1 + \delta_1 + \gamma_i + \eta_i + \kappa_i) + (\mu_1 + \kappa_i)(\mu_1 + \delta_1 + \gamma_i + \eta_i)], \\ \beta &= a\theta_i \frac{I_m}{N_h} [\delta_1(2\mu_1 + \delta_1 + \gamma_i + \eta_i) + (1 + \frac{S_i}{N_h})[(\mu_1 + \kappa_i)(\mu_1 + \delta_1 + \gamma_i + \eta_i) \\ &\quad + \mu_1(\mu_1 + \delta_1 + \gamma_i) + (3\mu_1 + \delta_1 + \gamma_i + \eta_i + \kappa_i)(2\mu_1 + \eta_i + \kappa_i)]], \\ \tau &= (a\theta_i \frac{I_m}{N_h})^2 (1 + \frac{S_i}{N_h}) [\delta_1 + (2\mu_1 + \eta_i + \kappa_i)(1 + \frac{S_i}{N_h})]. \end{aligned}$$

Proof. In (17), the resulting characteristic polynomial at IEE is given by

$$\lambda^3 + a_2\lambda^2 + a_1\lambda + a_0 = 0, \quad (20)$$

where

$$\begin{aligned} a_2 &= 3\mu_1 + \delta_1 + \gamma_i + \eta_i + \kappa_i + (1-p)a\theta_i \frac{I_m}{N_h} (1 + \frac{S_i}{N_h}), \\ a_1 &= (\mu_1 + \kappa_i)(\mu_1 + \delta_1 + \gamma_i + \eta_i) + \mu_1(2\mu_1 + \delta_1 + \gamma_i + \eta_i + \kappa_i) \\ &\quad + (1-p)a\theta_i \frac{I_m}{N_h} [\delta_1 + (2\mu_1 + \eta_i + \kappa_i)(1 + \frac{S_i}{N_h})], \\ a_0 &= \mu_1(\mu_1 + \kappa_i)(\mu_1 + \delta_1 + \gamma_i + \eta_i) + (1-p)a\theta_i \frac{I_m}{N_h} [\delta_1(\mu_1 + \kappa_i) + \mu_1(\mu_1 + \eta_i + \kappa_i)(1 + \frac{S_i}{N_h})]. \end{aligned}$$

We adopt Theorem 7.4 [15] to show the presence of purely imaginary roots in (20). For $R_i > 1$, we observe that the determinant $\Delta_1 = a_2 > 0$, $a_1 > 0$ and $a_0 > 0$ since all the parameters are positive. Now, Δ_2 can become zero from

$$\Delta_2 = a_2a_1 - a_0 = \alpha + \beta(1-p) + \tau(1-p)^2. \quad (21)$$

Let $p = p^*$ be a Hopf bifurcation parameter (and all other parameters of system(3) are fixed). Thus, $\Delta_2(p) = 0$ if and only if $p = p^*$. Hence,

$$\frac{\partial \Delta_2(p)}{\partial p} \Big|_{p=p^*} = -\beta - 2\tau(1-p^*) < 0.$$

Furthermore, it suffices to verify the transversality condition by showing that $\lambda = \varphi(p) + i\omega(p)$ is a solution to the cubic equation (20), and $\varphi(p) = 0$, then

$$\frac{\partial \varphi(p)}{\partial p} \Big|_{p=p^*} \neq 0.$$

To observe this, from (20) for $p = p^*$ and $\omega = \omega(p)$, we have

$$-i\omega^3 - a_2\omega^2 + ia_1\omega + a_0 = 0.$$

Isolating the real from the imaginary parts and equating each to zero gives

$$\omega^2 = a_1.$$

Differentiating the cubic equation(20) with respect to p at $p = p^*$ and $\lambda = i\omega$, we have

$$(-3\omega^2 + 2a_2i\omega + a_1)\frac{d\lambda}{dp} - \frac{\partial a_2}{\partial p}\omega^2 + \frac{\partial a_1}{\partial p}i\omega + \frac{\partial a_0}{\partial p} = 0.$$

Evaluating for $\frac{d\lambda}{dp}$ using $\omega^2 = a_1$, we get

$$\frac{d\lambda}{dp} \Big|_{p=p^*} = \frac{-a_1 \frac{\partial a_2}{\partial p} + \frac{\partial a_0}{\partial p} + i\sqrt{a_1} \frac{\partial a_1}{\partial p}}{2(a_1 - ia_2\sqrt{a_1})}. \tag{22}$$

Rationalizing the denominator in (22) and collecting the real parts after cancelling a_1 , we have

$$\frac{d\lambda}{dp} \Big|_{p=p^*} = \frac{-(\frac{\partial a_2 a_1}{\partial p} - \frac{\partial a_0}{\partial p})}{2(a_1 + a_2^2)} = \frac{-\frac{\partial \Delta_2}{\partial p}}{2(a_1 + a_2^2)} > 0.$$

Hence the proof. This is graphically given in Figure (3) below.

Next step of analysis focuses on the global dynamics of the model equilibria.

3.4. Global dynamics of the three-dimensional system 3.

Prop. 2. Assume that $p = 1$ and $R_i < 1$. Then the Infection-free equilibrium of the multi-system 1 is globally asymptotically stable.

Proof. Even though, construction of Lyapunov fuction does not follow any unified pattern, we took queue from the work of [28] to come up with a similar function

$$L_i^0 = S_i^0 \left(\frac{S_i}{S_i^0} - \ln \frac{S_i}{S_i^0} \right) + I_i + R_i$$

such that the time derivative gives

$$\begin{aligned} L_i^{0'}(t) &= \frac{dL_i}{dt} - \frac{S_i}{S_i^0} \frac{dL_i}{dt} + \frac{dI_i}{dt} + \frac{dR_i}{dt} \\ &= 2\Delta_i - \mu_1 S_i - \frac{\Delta_i^2}{\mu_1 S_i} + (1-p)a\theta_i \frac{I_m \Delta_i}{N_h \mu_1} - \left(\frac{\gamma_i \Delta_i}{\mu_1 S_i} + \mu_1 + \delta_1 \right) I_i \\ &\quad - \left(\frac{\kappa_i \Delta_i}{\mu_1 S_i} + \mu_1 \right) R_i \\ &= \Delta_i \left(2 - \frac{\mu_1 S_i}{\Delta_i} - \frac{\Delta_i}{\mu_1 S_i} \right) - \left(\frac{\gamma_i \Delta_i}{\mu_1 S_i} + \mu_1 + \delta_1 \right) I_i - \left(\frac{\kappa_i \Delta_i}{\mu_1 S_i} + \mu_1 \right) R_i \end{aligned}$$

(since $p = 1$).

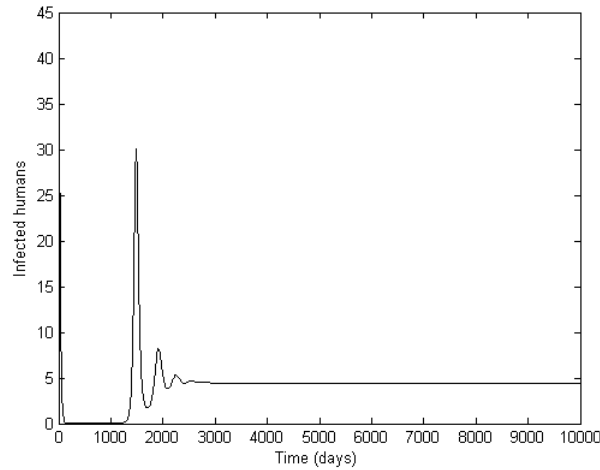


FIGURE 3. Simulation of the system(3) showing the total number of humans as a function of time. Parameter values used are: $a = 0.2; \theta_i = 1.5; \phi_i = 0.05; \gamma_i = 0.01; \delta_i = 0.7; \epsilon = 0.00005; \kappa_i = 1/(2 \times 365); \eta_i = 0.2; \mu_1 = 0.002; \mu_2 = 1/15; \delta_1 = 0.005; \delta_2 = 0.0005; \Delta_m = 500; p = p^* = 0.005$; such that $R_i = 4.734771277$. All other parameters as in Table 2

Clearly, $L_i^{0'}(t) < 0$ provided the geometric-arithmetic mean $2 - \frac{\mu_1 S_i}{\Delta_i} - \frac{\Delta_i}{\mu_1 S_i} \leq 0$. This shows that the infection-free equilibria E_i^0 are globally stable in the presence of maximum protection. The converse of the just concluded result explains that the persistence of mosquito bites for any kind of genotype possessed in human population may make the global eradication of malaria unrealistic.

Prop. 3. The unique infection endemic equilibrium of the three-dimensional system 3 is globally stable when $R_i > 1$ for each i .

Proof. Taking motivation from the work of [1], we adopt the famous quadratic Lyapunov function of the kind

$$V(x_1, x_2, \dots, x_n) = \sum_{j=1}^n \frac{c_j}{2} (x_j - x_j^*)^2. \quad (23)$$

from which the following main lyapunov function for the study is constructed

$$L_i(S_i, I_i, R_i) = \frac{1}{2} [(S_i - S_i^*) + (I_i - I_i^*) + (R_i - R_i^*)]^2. \quad (24)$$

The directional derivative of (24) alongside the solution curve of system (3) yields

$$L_i'(t) = [(S_i - S_i^*) + (I_i - I_i^*) + (R_i - R_i^*)] \frac{d}{dt} \sum_{i=1}^3 (S_i + I_i + R_i).$$

Using system (3), we obtain

$$L'_i(t) = [(S_i - S_i^*) + (I_i - I_i^*) + (R_i - R_i^*)][\Delta_i - \mu_i \sum_{i=1}^3 (S_i + L_i + R_i) - \delta_1 I_i].$$

and consequently, assuming that $\Delta_i = \mu_i \sum_{i=1}^3 (S_i^* + L_i^* + R_i^*)$ shows

$$L'_i(t) = [(S_i - S_i^*) + (I_i - I_i^*) + (R_i - R_i^*)][\mu_1 (S_i - S_i^*) + (\mu_1 + \delta_1)(I_i - I_i^*) + \mu_1 (R_i - R_i^*)].$$

Further simplification results to

$$\begin{aligned} L'_i(t) &= -\mu_i [(S_i - S_i^*)^2 + (R_i - R_i^*)^2] - (\mu_1 + \delta_1)(I_i - I_i^*)^2 \\ &\quad - 2\mu_1 (S_i - S_i^*)(R_i - R_i^*) - (2\mu_1 + \delta_1)(I_i - I_i^*)[(S_i - S_i^*) + (R_i - R_i^*)]. \end{aligned}$$

This illustrates that $L'_i(t) < 0$ and $L'_i(t) = 0$ provided $S_i = S_i^*, I_i = I_i^*$ and $R_i = R_i^*$. Thus, every solution of the system (3) approaches to the singleton set E_i^* as $t \rightarrow \infty$ which by La Salle invariance principle [11], the proof of the prop. 3 is concluded.

3.5. Global behaviour of the mosquito dynamics. The Lyapunov function used by [29] attracts our attention to investigate the global stability of the mosquito system 4 as so presented

$$L_m^0 = S_m + I_m$$

with the derivative defined by

$$\begin{aligned} L_m^{0'}(t) &= \frac{dS_m}{dt} + \frac{dI_m}{dt} \\ &= (\mu_2 + \delta_2) \left(\frac{\Delta_m}{\mu_2 + \delta_2} - 1 \right) I_m - \mu_2 S_m \\ &= (\mu_2 + \delta_2) (\Phi_m - 1) I_m - \mu_2 S_m \end{aligned}$$

Indeed, $L_m^{0'}(t) < 0$, if only if $\Phi_m \leq 1$ and $I_m = 0$. Thus, by the same principle as done in props. above, we can arrive at the next result.

Prop. 4 The infection-free equilibrium of the system 4 is globally asymptotically stable provided that $R_i^0 < 1$ and $\Phi_m \leq 1$.

Epidemiologically this implies that the control of malaria among the i genotype at the global level could be possible within the attraction zone assuming that the influx of mosquito population into the the community of humans is less than or equal to the sum of their death rates both natural and human induced.

3.6. Global behaviour of the model 4 at the infection endemic equilibrium. Despite many global methods at our disposal, we make use of Dulac's stability criterion to examine the global interior equilibrium at the infection endemic equilibrium of the model 4.

Prop.5 The global interior equilibrium of the model 4 has no closed orbits.
 Proof. As done in [30], we choose $D = \frac{1}{I_m}$ to be the Dulac's function and applying on

$$\left. \begin{aligned} f_m &= \Delta_m - (\mu_2 + \lambda_m)S_m, \\ g_m &= \lambda_m S_m - (\mu_2 + \delta_2)I_m, \end{aligned} \right\} \quad (25)$$

we see from (25) that

$$\begin{aligned} \frac{\partial Df_m}{\partial S_m} + \frac{\partial Dg_m}{\partial I_m} &= \frac{\mu_2}{I_m} - \frac{\lambda_m}{I_m} - \lambda_m \frac{S_m}{I_m^2} \\ &= -\left(\frac{\mu_2 + (1 + \frac{S_m}{I_m})\lambda_m}{I_m}\right) < 0, \end{aligned}$$

for $S_m \geq 0, I_m > 0$

which shows that there is no closed orbit within the sub-domain Ω_m according to the Bendixon -Dulac's theory.

4. NUMERICAL RESULTS AND DISCUSSIONS

Numerical simulations of the model (3) are carried out using a set of reasonable parameter values given in Table 2. We adopt a fourth-order Runge Kulta numerical scheme coded in Matlab for the numerical simulations.

TABLE 2. Parameter values of the extended model

Parameter	Value	Source
a	0.2	[18]
ϵ	0.00005	[18]
$(\theta_1, \theta_2, \theta_3)$	(0.05, 0.006, 0.0007)	[18]
(ϕ_1, ϕ_2, ϕ_3)	(0.05, 0.009, 0.0009)	[18]
$(\gamma_1, \gamma_2, \gamma_3)$	(0.033, 0.066, 0.132)	[18]
(μ_1, μ_2)	$(0.02, \frac{1}{15})$	[18]
(δ_1, δ_2)	0.005, 0.0005	[18]
$\Delta_i (i = 1, 2, 3)$	0.2	[18]
$\eta_i (i = 1, 2, 3)$	0.2	[18]
$\kappa_i (i = 1, 2, 3)$	$\frac{1}{730}$	[18]
Δ_m	500	[18]
p	[0, 1]	[variable]

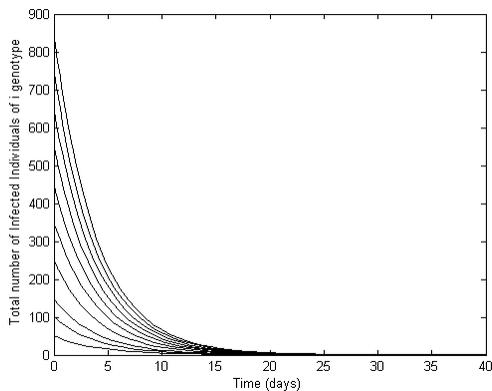


FIGURE 4. Simulation of the model 3 displaying the total number of infected individuals as a function of time for $R_i < 1$. Parameter values are as given in Table 2 with $\Delta_i = 0.7, \gamma_i = 0.2, \eta_i = 0, \phi_i = \theta_i = 0.05, p = 0.005$

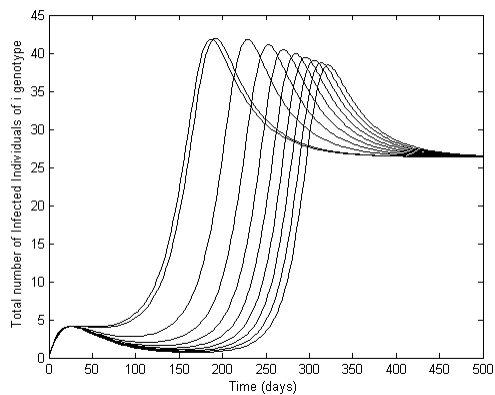


FIGURE 5. Simulation of the model 3 displaying the total number of infected individuals of i genotype as a function of time for $R_i > 1$. Parameter values are as given in Table 2 with $\Delta_i = 0.7, \gamma_i = 0.01, \eta_i = 0, \phi_i = \theta_i = 0.05, p = 0.005$

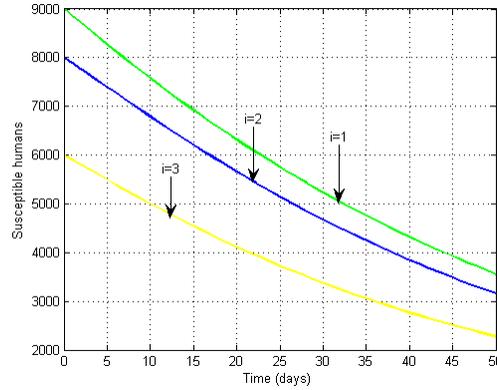


FIGURE 6. Simulation of the model 3 displaying the behaviour of susceptible dynamics as a function of time using parameter values in Table 2 with $\eta_i = 0, p = 0.005$

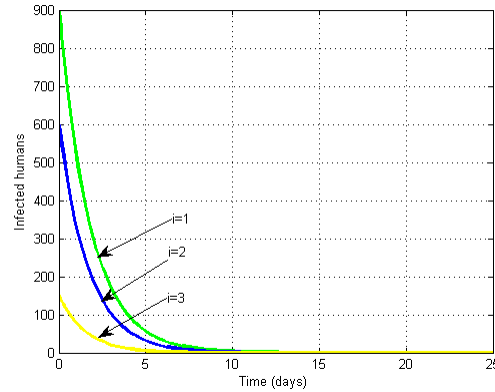


FIGURE 7. Simulation of the model 3 displaying the dynamics of AA ($i = 1$), AS ($i = 2$), and SS ($i = 3$) of infected individuals as a function of time using parameter values in Table 2 with $\eta_i \neq 0, p = 0.005$

Figure 4 describes the behaviour of the dynamics of malaria infected individuals of i genotype in the presence of treatment. The behaviour conforms to the analytical result globally since it converges to the infected free equilibrium. This means that AA, AS and SS individuals infected with malaria can be cured irrespective of initial conditions/ genetic status provided effective drugs are available and accessible for use.

Figure 5 illustrates the global convergence of the infected AA, AS and SS individuals at the infection endemic equilibrium when the basic reproduction number exceeds unity for the cases of no treatment. That means malaria infection can persist in both individuals of i genotype groups for a long time and thus both

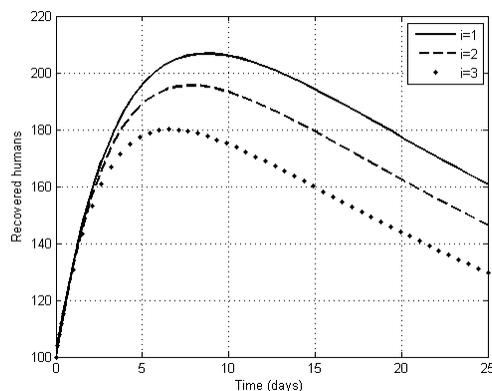


FIGURE 8. Simulation of the model 3 displaying the dynamics of recovered individuals as a function of time using parameter values in Table 2 with $\eta_i \neq 0, p = 0.005$

contribute to the endemicity of the disease

In Figure 6 the susceptibility behaviour of AA, AS and SS individuals in the presence of partial Immunity against malaria shows that SS genotype has the strongest immunity against malaria compare to AS and AA individuals. By implication AA genotype individuals are more vulnerable to malaria with AS being the second in order of contracting the disease. In literature, this result coincides with that of [19] that says S-allele inherited people are less candidates of plasmodium malaria.

In Figure 7: Here we observed that with proper treatment, the population of malaria-infected individuals of any genotype can be reduce adequately in numbers. However, SS infected population decreases in fewer days than those of AA and AS. This might be as a result of quick response to effective drugs and probably the early massive deaths related to malaria.

Figure 8 is a clear demonstration that all individuals irrespective of genetic status, who are infected of malaria recover from it. As notably observed AA ($i=1$), AS ($i=2$) recovers faster than the carrier ($i=3$) who are the least on the malaria recovery chart/figure. This outcome agrees with the work of [8] that says SS genotype individuals can survive to adulthood in high-income nations and even in malaria endemic settings as reported in [19]. Resistance to anti malaria drugs might have imbibe the recovery capacity of the sickle cell carriers. This particular outcome is in line with the earlier report of [10] on population genetics of malaria resistance in humans.

To study the effect of memory on the proposed model, the need to transform the system (3) into its fractional derivatives in the future becomes necessary and left open for incoming researchers.

5. CONCLUSION

A deterministic three-dimensional system for the transmission dynamics of malaria in a genetically stratified human population is designed and qualitatively studied. The basic model [18] is extended to incorporate a category of sickle cell carriers infected with malaria and also survived to adulthood. The extended model is shown to exhibit similar dynamics as the basic model except that it undergoes backward bifurcation, when the infection free equilibrium and infection endemic equilibrium co exist. By implication, the classical epidemiological requirement for the eradication of malaria when the basic reproduction number $R_i < 1$ is no longer sufficient, even though necessary. Quadratic equation method was used for the backward bifurcation analysis and the result represented graphically. The existence of a Hopf bifurcation is also investigated in the study. Furthermore, we derived conditions for the local and global stability of the infection-free equilibrium at $R_i < 1$ and the unique infection endemic equilibrium at $R_i > 1$ of the model. The case $R_i < 1$ shows that the malaria infection will be extinct gradually. The converse case will guarantee the persistence of the disease in the population. More so, a series of numerical simulations have been presented to show that the model agrees with the analytical results. Various numerical examples in the study reiterated that effective treatment can lead to malaria elimination in the community for any population irrespective of their genetic status. Our study also shows that even though sickle cell carriers are less candidates of malaria infection, their presence in the transmission dynamics has caused a significant effect even though little on the prevalence of the disease. This study importantly disclaimed the assertion that individuals with sickle cell gene do not recover from malaria and die before the reproduction age. We therefore, recommend that for complete malaria free society, individuals with double S-allele should equally be given attention in the control and treatment of the disease.

REFERENCES

- [1] J. K. K. Asamoah, F. N. M. Chand, H. Dutta, Mathematical Modelling of bacterial meningitis transmission dynamics with control measures. *Computational and Mathematical Methods in Medicine*, 2018, Article ID: 2657461, 21 pages
- [2] CDC, Malaria's Impact Worldwide. Accessed on July 29, 2020 from <https://www.cdc.gov/malaria/malaria-worldwide/impact.html>
- [3] P. Chanda-Kapata, M. Kapata, A. Zumla, COVID-19 and Malaria: A symptom screening challenge for malaria endemic countries. *International Journal of Infectious Diseases*, 94:151-153, 2020.
- [4] N. Chitnis, J. M. Hyman, J. M. Chusing, Determining important parameters in the spread of malaria through the sensitivity analysis of a mathematical model. *Bulletin of Mathematical Biology*, 70 (2008):1272-1296.
- [5] S. Eunha, Z. Feng, C. Castilo-Chavez, Differential impact of sickle cell trait on symptomatic and asymptomatic malaria. *Journal of Mathematical Biosciences and Engineering*, 9,4(2012): 877-898.
- [6] Z. Feng, Y. Yi, H. Zhu, Malaria epidemics and sickle cell gene dynamics. *Journal of Mathematical Biosciences*, 44,3(2002):174-180.
- [7] Z. Feng, Y. Yi, H. Zhu, Coupling ecology and evolution: Malaria and the S-genes across time scales. *Journal of Mathematical Biosciences*, 189(2004):1-19.
- [8] K. Gardner, A. Deuri, E. Drasar, N. Allman, A. Mwirigi, M. Awogbade, S. L. Thein, Survival in Adults with sickle cell disease in a high-income setting. *Letters to Blood*, 128,10(2016):1436-1438.

- [9] R. I. Gweryina, A.R. Kimbir, Dynamical behaviour of a malaria relapse model with insecticide treated nets (ITNs) as protection measure, *Applications and Applied Mathematics: An international Journal*, 15,1(2020):149-170.
- [10] P.W.Hedrick, Population genetics of malaria resistance in humans. *Heredity*, 107(2011):283-304.
- [11] J. P. La Salle, *The Stability of Dynamical Systems*. Hamilton Press, Berlin, New Jersey, USA, 70pp. 1976.
- [12] C. Liddell, N. Owusu-Brackett, D. Wallace, A mathematical model of sickle cell genome frequency in response to selective pressure from malaria. *Bulletin of Mathematical Biology*, 76,9(2014): DOI: 10.1007/s11538-014-9993-z
- [13] L. Luzzato, Sickle cell anaemia and malaria, *Mediterranean Journal of Haematology and Infectious Diseases*, 4,1(2012): e2012065, doi: 10.4084/MJHID.2012.065.
- [14] M. Martcheva, Methods for deriving necessary and sufficient conditions for backward bifurcation, *Journal of Biological Dynamics*, 13,1(2019):538-566.
- [15] M. Martcheva, *An Introduction to Mathematical Epidemiology*. Volume 61, New York: Springer Science and Business Media, pp.158-164, 2015.
- [16] A. E. Matouk, Complex Dynamics in Susceptible-Infected Models for COVID-19 with Multi-Drug Resistance. *Chaos, Solitons and Fractals*, 140, 110257, 2020.
- [17] C. C. McCluskey, P. Van den Driessche, Global analysis of two tuberculosis models. *Journal of Dynamics and Differential equations*, 16,1(2004):139-166.
- [18] J. Nakakawa, *Modelling Malaria and sickle cell gene*. Master's Thesis, Stellenbosch University <http://scholar.sun.ac.za>. 2011.
- [19] I. M. Okafor, H.U. Okoroiwu, C. A.Ekechi, Hameglobin S and Glucose-6-phosphate dehydrogenate deficiency co-inheritance in AS and SS individuals in malaria-endemic region: A study in Calabar, Nigeria. *Journal of Global Infectious Diseases*, (2011):118-22.
- [20] F. B. Piel, S. I. Hay, S. Gupta, D. J. Weatherall, T. N. Williams, Global burden of sickle cell Anaemia in children under five, 2010-2050: Modelling based on demographics, excess mortality, and interventions, *PLOS Medicine*, 10,7(2013):e100484. doi: 10.1371/journal.pmed.1001484.g001.
- [21] C. T. Quian, Z. R. Rogers, G. R. Buchanan, Survival of children with sickle cell disease, *Blood*, 103,11(2004):4023-4027.
- [22] Sickle Cell Society, Inheritance of sickle cell anaemia. Accessed on July 30, 2020, from <https://www.sicklecellsociety.org/resource/inheritance-sickle-cell-anaemia/>
- [23] F. Tluway, J. Makani, Sickle cell disease in Africa: An overview of the integrated approach to health, research, education and advocacy in Tanzania, 2004-2016. *BR. J. Haematol.* 177,6(2017):919-929.
- [24] J. Tumwine, J.Y.T. Mugisha, L.S. Luboobi, A mathematical model for the dynamics of malaria in a human host and mosquito vector with temporary immunity. *Applied Mathematics and Computation*, 189(2007):1953-1965.
- [25] P. Van den Driessche, and J. Watmough, Reproduction Numbers and Sub-Threshold Endemic Equilibria for Compartmental Models of Disease Transmission. *Journal of Mathematical Biosciences*, 180(2002): 29-48.
- [26] WHO, Sickle cell Anaemia. Fifty-Ninth World Health Assembly Provisional agenda item 11.4: A59/9, 2006
- [27] Y. Xiang, Z. Guo, J. Liu, Backward bifurcation in a malaria transmission model, *Journal of Biological Dynamics*, 14,1(2020):568-588.
- [28] H. Xiang, C. Zhu, H. Huo, Modelling the effect of immigration on drinking behaviour. *Journal of Biological Dynamics*, 11,1(2017):275-298.
- [29] X. Zhang, and B. Song, A bifurcation study on epidemic models with density-dependent treatments, *Mathematical and Theoretical Biology Institute (MTBI)*, Article Number: MTBI-10-07M, pp. 1-31. 2013.
- [30] H. Zhao, M. Zhao, Global hopf bifurcation analysis of an Susceptible-Infective-Removed epidemic model incorporating media coverage with time delay. *Journal of Biological Dynamics*, 11,1(2017):9-24.

R. I. GWERYINA

DEPARTMENT OF MATHEMATICS/STATISTICS/COMPUTER SCIENCE, FEDERAL UNIVERSITY OF AGRICULTURE, MAKURDI, NIGERIA

E-mail address: gweryina.reuben@uam.edu.ng

O. ABAH

DEPARTMENT OF MATHEMATICS/STATISTICS/COMPUTER SCIENCE, FEDERAL UNIVERSITY OF AGRICULTURE, MAKURDI, NIGERIA

E-mail address: onuabah@gmail.com

F. S. KADUNA

DEPARTMENT OF MATHEMATICS/STATISTICS/COMPUTER SCIENCE, FEDERAL UNIVERSITY OF AGRICULTURE, MAKURDI, NIGERIA

E-mail address: kadunafrancis@gmail.com